Proc. Natl. Acad. Sci. USA
Vol. 92, pp. 5194–5198, May 1995
Biochemistry

Identification of receptor-binding domains on human interleukin 5 and design of an interleukin 5-derived receptor antagonist

(cytokine receptor/solid-phase binding assay/proliferation assay/three-dimensional structure)

J. TAVERNIER*†, T. TUYPENS*, A. VERHEE*, G. PLAETINCK*, R. DEVOS*, J. VAN DER HEYDEN*, Y. GUISEZ*, and C. OEFNER‡

*Roche Research Gent, Jozef Plateaustraat 22, B-9000 Ghent, Belgium; and ‡Department of Pharmaceutical Research, New Technologies, F. Hoffmann–La Roche, Basel, Switzerland

Communicated by Marc Van Montagu, Universiteit Gent, Ghent, Belgium, February 6, 1995

ABSTRACT **A detailed structure–function analysis of human interleukin 5 (hIL5) has been performed. The hIL5 receptor is composed of two different polypeptide chains, the α and β subunits. The α subunit alone is sufficient for ligand binding, but association with the β subunit leads to a 2- to 3-fold increase in binding affinity. The β chain is shared with the receptors for IL3 and granulocyte/macrophage-colony-stimulating factor—hence the descriptor β_C (C for common). All hIL5 mutants were analyzed in a solid-phase binding assay for hIL5Rα interaction and in a proliferation assay using IL5-dependent cell lines for receptor-complex activation. Most residues affecting binding to the receptor α subunit were clustered in a loop connecting β-strand 1 and helix B (mutants H38A, K39A, and H41A), in β-strand 2 (E89A and R91A; weaker effect for E90A) and close to the C terminus (T109A, E110A, W111S, and I112A). Mutations at one position, E13 (Glu^{13}), caused a reduced activation of the hIL5 receptor complex. In the case of E13Q, only 0.05% bioactivity was detected on a hIL5-responsive subclone of the mouse promyelocytic cell line FDC-P1. Moreover, on hIL5-responsive TF1 cells, the same mutant was completely inactive and proved to have antagonistic properties. Interactions of this mutant with both receptor subunits were nevertheless indistinguishable from those of nonmutated hIL5 by crosslinking and Scatchard plot analysis of transfected COS-1 cells.**

Human interleukin 5 (hIL5) is a disulfide-linked homodimeric glycoprotein with 115 aa per monomer (1) and has been produced in various heterologous systems (2–4). Analysis of the glycosylation pattern of Chinese hamster ovary (CHO) cell-derived IL5 revealed an antiparallel dimer linkage. Also, hIL5 was found to have O-linked glycosylation at Thr-3 (T3) and N-linked glycosylation at Asn-28 (N28) (5), but deglycosylation did not affect the biological activity (2). The structure of IL5 purified from *Escherichia coli* (6) and Sf9 cells (ref. 7; see Fig. 5) has been determined. hIL5 adopts the typical four α-helical bundle "cytokine fold" which has also been described for other cytokines, including granulocyte/macrophage-colony-stimulating factor (GM-CSF), IL2, IL4, macrophage-colony-stimulating factor, and growth hormone (GH). This fold consists of a bundle of four α-helices in an up–up, down–down array. Unique to IL5, however, is the phenomenon of D-helix swapping, whereby one bundle is built up of three helices coming from one monomer and a fourth helix which is contributed by the second monomer. In addition to the four α-helical bundle, hIL5 also contains two short antiparallel β-strands located between helices A and B and helices C and D.

The human as well as the mouse IL5 receptor (IL5R) consists of two different chains, the α and β subunits (8–13). hIL5 binds to the α subunit with intermediate affinity (K_d = 4×10^{-10} M; equivalent to the low-affinity binding site in the mouse), which is increased 2- to 3-fold upon association with the β chain. This β subunit is shared with GM-CSF and IL3, which explains the overlap of biological activities observed for these cytokines (8, 14, 15). Accordingly, cell type-specific expression of the α subunit (i.e., in eosinophils and basophils in the case of hIL5) restricts the activity repertoire to that cell type. We have reported that mature eosinophils express predominantly an mRNA encoding a soluble human IL5R α-subunit (shIL5Rα) variant which has antagonistic properties *in vitro* (8). This and another, very similar, minor variant arise from splicing variation (16, 17). Remarkably, one hIL5 homodimer binds only one soluble isoform in solution (18).

Little is known about the structure–activity relationship of IL5. A role for the C-terminal 36 residues has been inferred from species-specificity studies using human/mouse chimeric polypeptides (19). In another study, C-terminal amino acids were also implicated in biological activity (20). Here, we report a detailed mutagenesis analysis and the development of an antagonistic IL5 mutein.

MATERIALS AND METHODS

Site-Specific Mutagenesis and Expression. Mutations were introduced into the hIL5 polypeptide by an adapted protocol using a commercially available kit (Transformer; Clontech). Plasmid DNAs harboring the mutant IL5 genes were introduced into the *Autographa californica* nuclear polyhedrosis virus genome by cotransfection with linearized baculovirus DNA in Sf9 cells (Baculogold; PharMingen). To avoid cross-contamination of virus stocks, pipetting was done with active-displacement pipettes in a laminar-flow bench. Recombinant baculovirus amplification, mutant hIL5 production, and [^{35}S]methionine labeling of hIL5 mutants was performed essentially as described (2).

Immunodetection of hIL5 Mutants. Two different ELISAs were used to quantitate hIL5 muteins. In a first assay, immunoplates (Nunc) were coated with H30, a rat non-neutralizing monoclonal antibody (mAb) against hIL5. Serial dilutions of IL5 (mutant) samples were added, followed by mouse anti-hIL5 mAb (1F1 or 4G5) and then horseradish peroxidase-conjugated anti-mouse immunoglobulin antibody. The second ELISA was set up using 5A5, a mouse neutralizing anti-hIL5 mAb. This mAb was used both as coating and as second antibody (conjugated with horseradish peroxidase), taking advantage of the dimeric structure of IL5. In one case, mutant R90A (Arg-90 → Ala), the ELISA used mAbs 1F1 and 4G5.

The publication costs of this article were defrayed in part by page charge payment. This article must therefore be hereby marked "*advertisement*" in accordance with 18 U.S.C. §1734 solely to indicate this fact.

Abbreviations: IL*n*, interleukin *n*; IL*n*R, IL*n* receptor; GM-CSF, granulocyte/macrophage-colony-stimulating factor; GH, growth hormone; GHR, GH receptor; prefix h, human; prefix s, soluble; mAb, monoclonal antibody.

†To whom reprint requests should be addressed.

Analysis of Receptor Interactions of hIL5 Mutants. The effect of mutations on hIL5Rα binding was monitored separately in a solid-phase binding assay (18). Probind plates (Becton Dickinson) were coated with polyclonal goat anti-hIgG and loaded with shIL5Rα-hIgG3 fusion protein. Then a competition assay was performed by applying serial dilutions of Sf9 supernatants containing hIL5 muteins together with a fixed amount of ^{125}I-labeled hIL5. All mutants were also tested in two different bioassays. First, proliferative activity was monitored with hIL5-dependent FDCP1-CA1 cells. This cell line was derived from FDC-P1 cells by introducing hIL5Rα cDNA (S. Cornelis, J.V.d.H., J.T., and G.P., unpublished work). In most cases, hIL5 muteins were also tested on TF1-hIL5Rα cells, a hIL5-dependent derivative of the human erythroleukemia cell line TF-1 (ref. 21; here too, hIL5 responsiveness was obtained after stable transfection of cDNA encoding hIL5Rα). Cells were seeded in the presence of serial dilutions of hIL5 (mutant) polypeptides at 1000 or 3000 cells per well for FDCP1-CA1 and TF1-hIL5Rα cells, respectively,

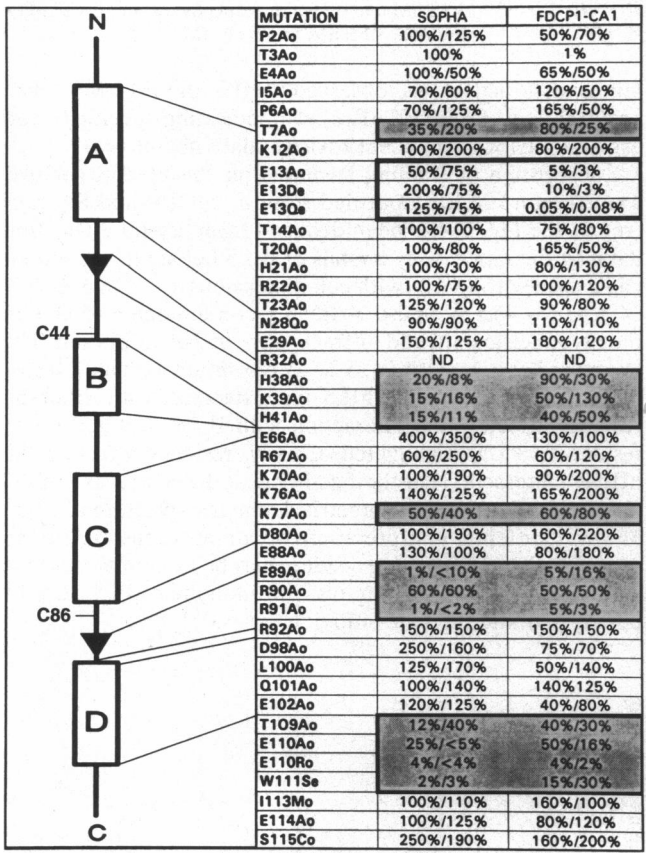

MUTATION	A SOPHA	B FDCP1-CA1
P2Ao	100%/125%	50%/70%
T3Ao	100%	1%
E4Ao	100%/50%	65%/50%
I5Ao	70%/60%	120%/50%
P6Ao	70%/125%	165%/50%
T7Ao	35%/20%	80%/25%
K12Ao	100%/200%	80%/200%
E13Ao	50%/75%	5%/3%
E13De	200%/75%	10%/3%
E13Qe	125%/75%	0.05%/0.08%
T14Ao	100%/100%	75%/80%
T20Ao	100%/80%	165%/50%
H21Ao	100%/30%	80%/130%
R22Ao	100%/75%	100%/120%
T23Ao	125%/120%	90%/80%
N28Qo	90%/90%	110%/110%
E29Ao	150%/125%	180%/120%
R32Ao	ND	ND
H38Ao	20%/8%	90%/30%
K39Ao	15%/16%	50%/130%
H41Ao	15%/11%	40%/50%
E66Ao	400%/350%	130%/100%
R67Ao	60%/250%	60%/120%
K70Ao	100%/190%	90%/200%
K76Ao	140%/125%	165%/200%
K77Ao	50%/40%	60%/80%
D80Ao	100%/190%	160%/220%
E88Ao	130%/100%	80%/180%
E89Ao	1%/<10%	5%/16%
R90Ao	60%/60%	50%/50%
R91Ao	1%/<2%	5%/3%
R92Ao	150%/150%	150%/150%
D98Ao	250%/160%	75%/70%
L100Ao	125%/170%	50%/140%
Q101Ao	100%/140%	140%125%
E102Ao	120%/125%	40%/80%
T109Ao	12%/40%	40%/30%
E110Ao	25%/<5%	50%/16%
E110Ro	4%/<4%	4%/2%
W111Se	2%/3%	15%/30%
I113Mo	100%/110%	160%/100%
E114Ao	100%/125%	80%/120%
S115Co	250%/190%	160%/200%

FIG. 1. Characterization of the receptor binding and biological properties of hIL5 muteins. At the left, the structure of one hIL5 monomer is shown in lines (random coils), open boxes (α-helices), and arrows (β-strands). The N and C termini are indicated. The location of the secondary structure elements is derived from x-ray crystallography data (ref. 6; see Fig. 5). Positions of selected mutations are indicated by dashed lines; o and e at the ends of mutant names indicate that *Nco* I and *Nde* I restriction sites were used in mutagenesis selection. All hIL5 mutants were analyzed in a solid-phase binding assay (column A, SOPHA) and in a proliferation assay using FDCP1-CA1 cells (column B). All mutants were analyzed twice in two independent experiments and data are expressed as percent activity vs. wild-type hIL5. In all cases, with the only exception being the E13 mutants, maximum proliferation levels were comparable to those seen with wild-type hIL5. Mutants affecting the hIL5Rα interaction showed a leftward shift in the dose–response curves and are indicated by shading. Mutants affecting receptor activation without any reduced hIL5Rα binding are boxed.

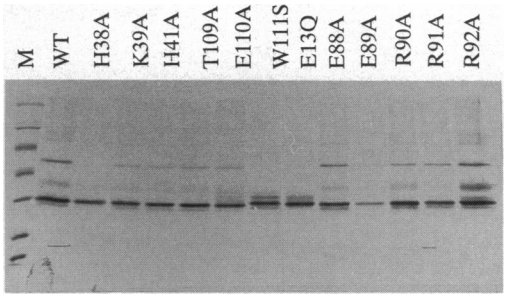

FIG. 2. [^{35}S]Methionine labeling of hIL5 mutants. Shown is an autoradiograph of a selection of hIL5 mutants obtained after internal labeling with [^{35}S]methionine and subsequent immunoprecipitation and SDS/15% PAGE. Mutations are indicated on top of each lane. IL5 was detected as a dimer because the gel was run under nonreducing conditions. M, size markers (200, 97, 69, 46, 30, 21, and 14 kDa); WT, wild-type hIL5.

and proliferation was measured after 65 hr by [^{3}H]thymidine incorporation for 4–5 hr. Crosslinking and Scatchard plot analysis were performed as described (8).

RESULTS

IL5 Mutagenesis and Expression. hIL5 mutations included an almost complete alanine scan (individual replacement by alanine) of the charged residues, (only some residues between C44 and helix B and between helix C and C86 were omitted), followed by a more detailed analysis of the N and C termini (Fig. 1). The IL5 mutants were generated in pVL941-hIL5 and expressed in Sf9 cells as described (2). Expression was monitored by metabolic labeling with [^{35}S]methionine followed by immunoprecipitation with an anti-hIL5 polyclonal antibody and SDS/PAGE (Fig. 2). In addition, more accurate quantification was performed with two different ELISAs using hIL5-specific mAbs. These analyses confirmed structural integrity of the mutant proteins and identified the binding epitopes of these mAbs (J.V.d.H., T.T., R.D., G.P., X. Van Ostade, Y.G., and J.T., unpublished work). Whenever relevant, tests were performed to check the stability of the mutant proteins (see below).

Identification of Residues Affecting IL5Rα Binding and IL5R Activation. All mutants were tested in two different assay systems. First, a hIL5Rα-specific solid-phase binding assay was performed (18). In brief, a soluble hIL5Rα-hIgG3 fusion protein was fixed on anti-hIgG-coated plates and used to analyze ^{125}I-hIL5 binding in the presence of the hIL5 mutants in a competition experiment (Fig. 1, column A). Second, the hIL5 mutants were tested for their biological activity in a proliferation assay using hIL5-dependent FDCP1-CA1 and TF1-hIL5Rα cell lines. These cell lines were obtained after stable expression of hIL5Rα. In addition to mutations interfering with hIL5Rα binding, activation of the receptor complex was also monitored. Such activation requires the presence of the β_C subunit (which is AIC2B in the case of the FDC-P1 subclone) in the complex. Properties of the mutants in the FDCP1-CA1 assay are given in Fig. 1, column B.

Most mutations affecting the IL5Rα interaction, as identified in the solid-phase binding assay, also resulted in reduced activity in the proliferation assays (e.g., E89A, R91A, E110A, and W111S). In addition, however, some weakly positive mutants (e.g., H38A, K39A, and H41A) could be selected only in the solid-phase binding assay. This indicates that, although the bioassay is much more sensitive, a slightly reduced affinity for the IL5Rα does not necessarily lead to a decreased specific biological activity. Indeed, it is very likely that a somewhat reduced receptor occupancy will still evoke a full biological response in a cell-based assay. Hence it appears that, in

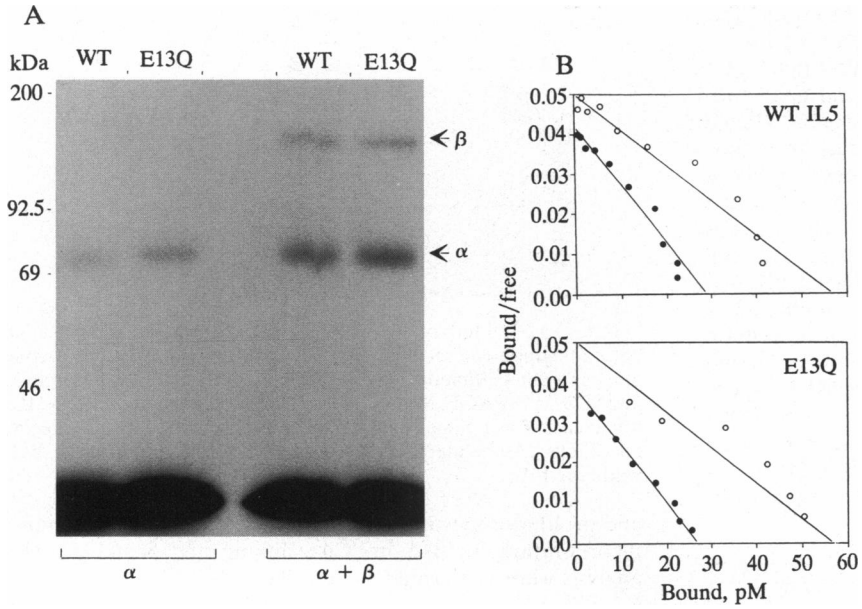

FIG. 3. Crosslinking and Scatchard analysis of mutant E13Q. (*A*) Crosslinking of radiolabeled wild-type hIL5 (WT) or mutant E13Q on COS-1 cells transfected with hIL5Rα cDNA (α) or cells cotransfected with α- and β_C-chain cDNA (α + β). Positions of crosslinked α and β chains are indicated. (*B*) Scatchard analysis of binding of ^{125}I-labeled wild-type (WT) hIL5 (*Upper*) or E13Q (*Lower*) on COS-1 cells expressing hIL5Rα alone (○) or hIL5Rα together with β_C chain (●). The calculated K_d values for binding of WT on α-expressing cells and α/β-expressing cells were 1.12 nM and 0.59 nM, respectively, and for E13Q binding, 1.55 nM and 0.65 nM.

assessing the reduced level of binding, the solid-phase binding assay is ≈5-fold more accurate than the bioassays. In all cases where the interaction with IL5Rα was affected, we observed a leftward shift in the dose–response curve. No effect on the maximal binding or proliferation level was observed. In summary, residues where mutations affect IL5Rα interaction are located in β-strand 2 (residues E89 and R91; weaker effect at E90), in the loop between β-strand 1 and helix B (H38, K39, and H41), and at the end of helix D (T109, E110, W111, and I112). Weak effects were also observed at positions 7 (T7A) and 77 (K77A). In one case, mutant E66A in the solid phase binding assay, we noted a potential enhanced interaction with IL5Rα.

Two mutants scored as wild-type hIL5 in the solid-phase binding assay but showed a marked decrease in the proliferation assay: T3A and E13A (respectively 1% and 5% activity relative to wild-type IL5). Such a phenotype would correspond to mutants with a reduced efficiency in receptor activation. However, an alternative explanation for a reduced activity in the bioassay (3-day incubation at 37°C) versus the solid-phase binding assay (1-hr incubation at room temperature), could be a decreased stability of the mutant proteins. To assess this possibility, mutants were preincubated under bioassay conditions and subsequently checked for remaining activity in the solid-phase binding assay. The activity of mutant T3A was indeed strongly reduced, but mutant E13A appeared to be stable (data not shown). Analysis of two additional mutants at this position, E13D and E13Q, confirmed this observation, as these only had 10% and 0.05% proliferative activity left, respectively.

Antagonistic Properties of Mutant E13Q. Mutant E13Q was analyzed in more detail. Scatchard plot analysis of mutant E13Q is shown in Fig. 3*B*. Binding affinities were measured on COS-1 cells transiently expressing hIL5Rα either alone or coexpressed with the β_C chain. Surprisingly, the E13Q mutein was indistinguishable from wild-type hIL5 for both binding to the hIL5Rα subunit and for affinity conversion upon interaction with β_C. Confirming this result, crosslinking revealed the presence of a β chain in the complex for both the E13Q mutein and wild-type hIL5 (Fig. 3*A*).

Although mutant E13Q had residual activity when assayed on the FDCP1-CA1 subclone (see above), no proliferative response was detectable on TF1-hIL5Rα cells, even at an E13Q concentration of 150 μg/ml. Further, this variant had antagonistic properties (Fig. 4). The IC_{50} was 30 ng/ml, which represents a 60-fold molar excess over wild-type hIL5. No antagonistic activity was observed for IL3- or GM-CSF-driven proliferation of TF1-hIL5Rα cells, indicating specificity and excluding E13Q-dependent toxicity (data not shown).

Localization of Binding Domains on the hIL5 Structure. The structure of hIL5 purified from *E. coli* (6) and Sf9 cells (ref. 7; see Fig. 5) has been deduced from crystal diffraction data. In the latter case, crystals of hIL5 belong to the monoclinic space group *C*2 (with cell dimensions a = 118.6 Å, b = 24.4 Å, c = 45.5 Å, and β = 109.2°), contain one molecule in the asymmetric unit, and diffract to about 2-Å resolution. The structure has been refined to 2.5-Å resolution with an R factor of 14.3%. Fig. 5 shows the hIL5 dimer structure with either the residues affecting the interaction with IL5Rα (*B* and *C*) or residue E13 (*D*) highlighted. Clearly, residues affecting the hIL5Rα interaction cluster together near the central axis of the IL5 dimer. Due to the symmetrical, dimeric structure of hIL5, however, different interpretations of our mutagenesis data can be given; all the interacting residues may be located on one side of the dimer (Fig. 5*B*) or on one monomer (Fig. 5*C*), or perhaps an intermediate situation exists.

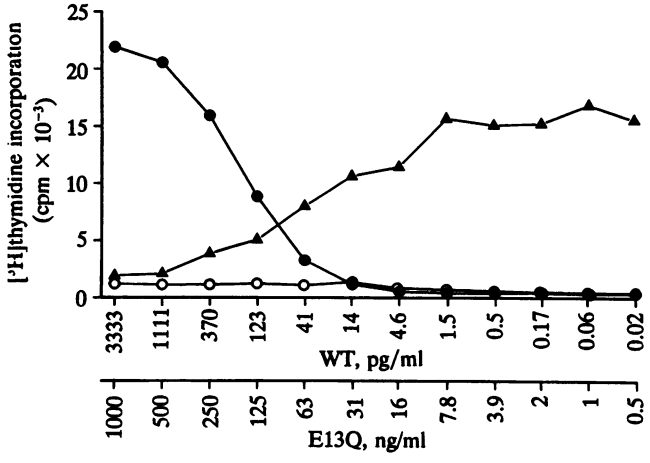

FIG. 4. E13Q antagonism on TF1-hIL5Rα cells. TF1-hIL5Rα cell proliferation was measured by [^{3}H]thymidine incorporation for serial dilutions of wild-type (WT) hIL5 (1:3, ●, starting at 3.3 ng/ml) and mutant E13Q (1:2, ○, starting at 1000 ng/ml). ▲, Proliferation in the presence of 500 pg of wild-type hIL5 (1 unit) in each well, supplemented with a serial dilution of E13Q as above.

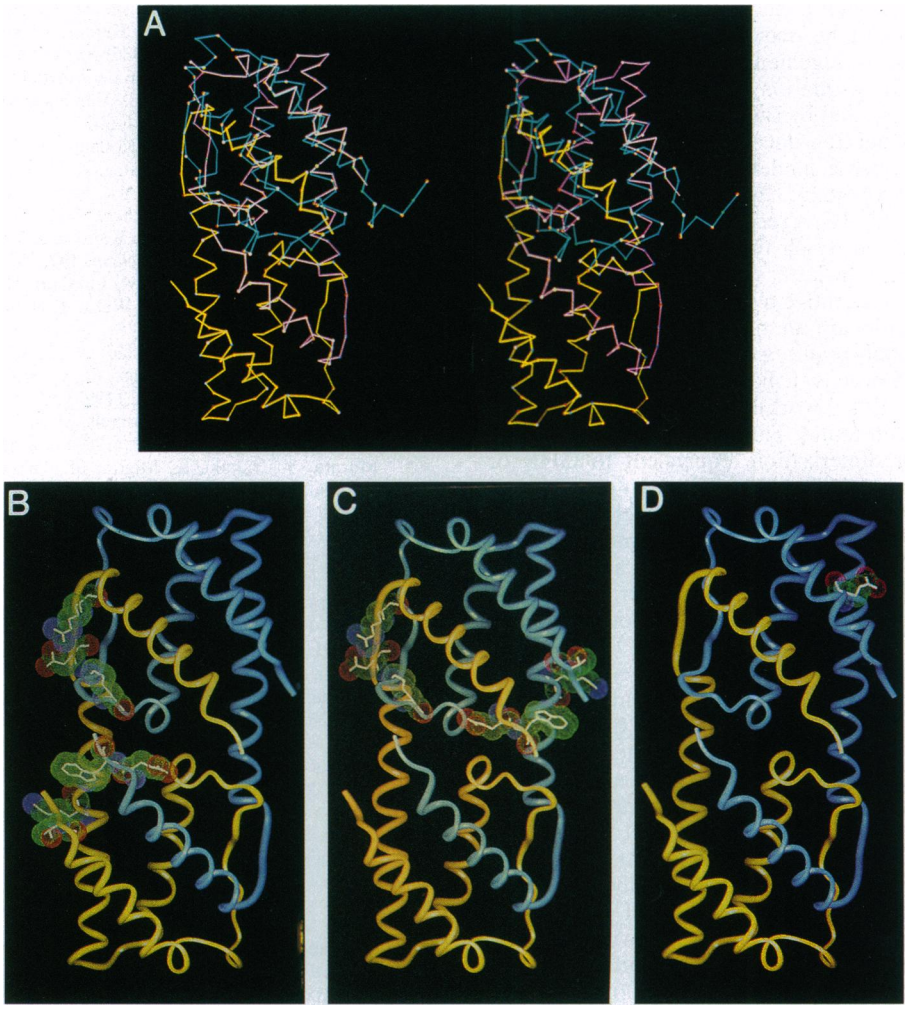

FIG. 5. Structure of hIL5 and localization of hIL5 mutants. (*A*) Stereo representation of the C^{α} backbone of the crystallographic hIL5 dimer, viewed along the twofold axis of symmetry. The two monomers are shown in yellow and cyan, respectively. Shown in magenta is the C^{α} backbone of hGM-CSF as deposited in the Brookhaven Protein Databank (1GMF) superimposed onto one hIL5 monomer after a least-squares fit of 44 equivalent α-helical C^{α} positions. The root-mean-square deviation is 1.7 Å. (*B* and *C*) Localization of hIL5Rα mutants. Mutants affecting hIL5Rα interaction are shown by their van der Waals radii. hIL5 mutants are depicted at one side of the hIL5 dimer (*B*) or on one monomer (*C*). (*D*) Localization of position E13.

DISCUSSION

The first requirement for receptor triggering is the binding of hIL5 to hIL5Rα. By testing a series of site-specific mutations in the ligand in a solid-phase binding assay, residues involved in α-subunit interaction have been identified. The mutants cluster around the dimer interface belonging either to one or to both monomers (Fig. 5). Due to the twofold symmetry of the dimeric IL5 structure, analysis of heterodimers in which different mutations are combined will be required to find out whether the IL5Rα binding site is formed by one or by both monomers or whether an intermediate situation is present. Nonetheless, we can deduce that the area which interacts with the receptor α-subunit is located near the central symmetry axis of the dimer. This interpretation is confirmed by the location of the overlapping epitopes of a non-neutralizing (H30) and a neutralizing (5A5) mAb, which bind either apically or to the central axis of the outer β-strand (residues 90–92 and residues 89–91, respectively; J.V.d.H., T.T., R.D., G.P., X. Van Ostade, Y.G., and J.T., unpublished work).

According to the structure of the ligand/receptor complex of human GH, a member of the α-helical cytokine family, which has been determined (22), it can be argued that the hIL5Rα interaction site is spread over the dimer interface (as shown in Fig. 5*B*). In the case of human GH, one monomer interacts sequentially with two identical GH receptor (GHR) molecules (23). Residues involved in the first interaction site (I) are mainly located on helix D as well as in the loop between helices A and B, identifying one side of the GH monomer. The distance between residues forming site I is ≈35 Å. Assuming that hIL5Rα (which consists of three fibronectin III-like modules, compared with only two for GHR; ref. 17) has a footprint of at least equal size on the hIL5 dimer, one could deduce that most of the central part of the hIL5 dimer and hence residues from both monomers should contribute to receptor binding (in Fig. 5*B*, the distance along the twofold axis between residues forming the hIL5Rα interaction site is 32 Å). Interactions over the interface of ligand subunits are not exceptional and have been described before—e.g., for tumor necrosis factor (24, 25). Considering the high degree of structural similarity between hIL5 and hGM-CSF (Fig. 5*A*), one might ask whether the related cytokines GM-CSF and IL-3 might also need to dimerize upon interaction with their respective receptor α subunits. The more pronounced affinity conversion observed for these cytokines (20-fold and 1000-fold for GM-CSF and IL-3, respectively) might be caused mainly by

such dimerization event with concomitant increase in α-subunit binding, in addition to the association with the β_C subunit.

The stoichiometry of engagement of the β_C subunit in the complex is unclear. The formation of an $\alpha\beta_C\beta_C$ complex for GM-CSF has been suggested by Budel *et al.* (26), and dimerization of the gp130 signal transducer in the IL6R complex has been described (27). Such a model is also supported by the observation that erythropoietin, (Epo)-mediated crosslinking of two chimeric mEpoR/AIC2A receptors (AIC2A is a murine β-subunit homologue), in which the former contributes the extracellular domain and the latter the intracellular domain, is sufficient to evoke a proliferative response (28). In contrast to sIL6R, shIL5Rα subunits are antagonistic (8), and the complete hIL5Rα is absolutely required for signaling (29) and Jak2 kinase activation (S. Cornelis, I. Faché, J.V.d.H., Y.G., J.T., R.D., and G.P., unpublished work). In addition, no evidence for a β_C dimer has been found. Thus, activation of the IL5R complex by $\alpha\beta$ heterodimerization, equivalent to GHR or gp130 homodimerization, cannot be ruled out at present. It is also still unclear why the IL5 dimer does not interact with two α chains. Perhaps steric hindrance or a conformational shift in the IL5 dimer induced upon interaction with an α subunit causes the interaction with the β chain. Alternatively, the receptor might already exist as a preformed $\alpha\beta$ complex on the cell membrane (30).

Mutations at residue 13 affected receptor activation without reducing hIL5Rα binding. Moreover, on TF1-hIL5Rα cells, the proliferative activity was abolished and the E13Q mutein behaved as a potent receptor antagonist. We next examined the interaction with the β_C subunit. Homologous positions in GM-CSF (E21) and in IL3 (E22) have been reported to affect the interaction with this shared β_C subunit (31–33). Such a negatively charged residue is present at a similar location for almost all members of the helical cytokine family. Suggesting an analogy between the IL5/IL5R and the GH/GHR interactions, the location of residue E13 agrees well with the GHR site II, both being located on helix A. To our surprise, however, both Scatchard plot analysis and crosslinking on transfected COS-1 cells showed no differential behavior between this mutant and wild-type hIL5 (Fig. 3). Perhaps the E13Q mutein is incapable of engaging a second β_C subunit in the complex, is defective in inducing allosteric shifts required to activate the $\alpha\beta$ receptor complex, or both. Presently we cannot discriminate between these possibilities. The absence of quantitative differences in the crosslinking experiment described in Fig. 3*A* might support an $\alpha\beta_C$ induced-fit model. The identification of a biologically active murine GM-CSF E22A mutein which binds to its receptor complex with low affinity only, despite the presence of the β_C subunit (34), can be explained by each of these models. Taken together, these mutant studies clearly show that affinity conversion and receptor activation can be uncoupled.

It has been documented for the GHR complex that direct interactions between the receptor subunits may be involved in receptor complex formation and stabilization. Perhaps ligand-induced allosteric shifts in the receptor structures might contribute to such direct interactions of receptor subunits ($\alpha\beta_C$ hetero- or β_C homodimerization). In this receptor class, no agonistic antibodies have been described. Answers to these questions will require the elucidation of the three-dimensional structure of the receptor subunits and of the ligand/receptor complex.

We gratefully acknowledge the excellent technical assistance of Ina Faché, Freya Van Houtte, and Johan Bostoen. We thank Dr. Xaveer Van Ostade and Dr. Harald Gallatti for help with the H30 and 5A5 ELISAs, respectively, and Didier Moens for assistance in computer modeling. Throughout the course of this work, we appreciated the many suggestions of Prof. Colin Sanderson, Dr. Angel Lopez, and Dr. Sigrid Cornelis. Finally, we are also greatly indebted to Prof. Walter Fiers, Dr. Michael Steinmetz, and Dr. Ann Welton for helpful discussions.

1. Azuma, C., Tanabe, T., Konishi, M., Kinashi, T., Noma, T., Matsuda, F., Yaoita, Y., Takatsu, K., Hammarström, L., Smith, C. I. E., Severinson, E. & Honjo, T. (1986) *Nucleic Acids Res.* **14,** 9149–9158.
2. Tavernier, J., Devos, R., Van der Heyden, J., Hauquier, G., Bauden, R., Faché, I., Kawashima, E., Vandekerckhove, J., Contreras, R. & Fiers, W. (1989) *DNA* **8,** 491–501.
3. Tsujimoto, M., Adachi, H., Kodama, N., Tsuruoka, N., Yamada, Y., Tanaka, S., Mita, S. & Takatsu, K. (1989) *J. Biochem.* **106,** 23–28.
4. Proudfoot, A. E. I., Fattah, D., Kawashima, E. H., Bernard, A. & Wingfield, P. T. (1990) *Biochem. J.* **270,** 357–361.
5. Minamitake, Y., Kodama, S., Katayama, T., Adachi, H., Tanaka, S. & Tsujimoto, M. (1990) *J. Biochem.* **107,** 292–297.
6. Milburn, M. V., Hassell, A. M., Lambert, M. H., Jordan, S. R., Proudfoot, A. E. I., Graber, P. & Wells, T. N. C. (1993) *Nature (London)* **363,** 172–176.
7. Guisez, Y., Oefner, C., Winkler, F. K., Schlaeger, E.-J., Zulauf, M., Van der Heyden, J., Plaetinck, G., Cornelis, S., Tavernier, J., Fiers, W., Devos, R. & D'Arcy, A. (1993) *FEBS Lett.* **331,** 49–52.
8. Tavernier, J., Devos, R., Cornelis, S., Tuypens, T., Van der Heyden, J., Fiers, W. & Plaetinck, G. (1991) *Cell* **66,** 1175–1184.
9. Murata, Y., Takaki, S., Migita, M., Kikuchi, Y., Tominaga, A. & Takatsu, K. (1992) *J. Exp. Med.* **175,** 341–351.
10. Takaki, S., Tominaga, A., Hitoshi, Y., Mita, S., Sonoda, E., Yamaguchi, N. & Takatsu, K. (1990) *EMBO J.* **9,** 4367–4374.
11. Devos, R., Vandekerckhove, J., Rolink, A., Plaetinck, G., Van der Heyden, J., Fiers, W. & Tavernier, J. (1991) *Eur. J. Immunol.* **21,** 1315–1317.
12. Devos, R., Plaetinck, G., Van der Heyden, J., Cornelis, S., Vandekerckhove, J., Fiers, W. & Tavernier, J. (1991) *EMBO J.* **10,** 2133–2137.
13. Takaki, S., Mita, S., Kitamura, T., Yonehara, S., Yamaguchi, N., Tominaga, A., Miyajima, A. & Takatsu, K. (1991) *EMBO J.* **10,** 2833–2838.
14. Kitamura, T., Sato, N., Arai, K.-I. & Miyajima, A. (1991) *Cell* **66,** 1165–1174.
15. Lopez, A., Eglinton, J. M., Gillis, D., Park, L. S., Clark, S. & Vadas, M. A. (1989) *Proc. Natl. Acad. Sci. USA* **86,** 7022–7026.
16. Tavernier, J., Tuypens, T., Plaetinck, G., Verhee, A., Fiers, W. & Devos, R. (1992) *Proc. Natl. Acad. Sci. USA* **89,** 7041–7045.
17. Tuypens, T., Plaetinck, G., Baker, E., Sutherland, G., Brusselle, G., Fiers, W., Devos, R. & Tavernier, J. (1992) *Eur. Cytokine Netw.* **3,** 451–459.
18. Devos, R., Guisez, Y., Cornelis, S., Verhee, A., Van der Heyden, J., Manneberg, M., Lahm, H.-W., Fiers, W., Tavernier, J. & Plaetinck, G. (1993) *J. Biol. Chem.* **9,** 6581–6587.
19. McKenzie, A. N. J., Barry, S. C., Strath, M. & Sanderson, C. J. (1991) *EMBO. J.* **10,** 1193–1199.
20. Kodama, S., Tsuruoka, N. & Tsujimoto, M. (1991) *Biochem. Biophys. Res. Commun.* **178,** 514–519.
21. Kitamura, T., Tange, T., Terasawa, T., Chiba, S., Kuwaki, T., Miyagawa, K., Piao, Y., Miyazono, K., Urabe, A. & Takaku, F. (1989) *J. Cell. Physiol.* **140,** 323–334.
22. de Vos, A. M., Ultsch, M. & Kossiakoff, A. A. (1992) *Science* **255,** 306–312.
23. Cunningham, B. C., Ultsch, M., de Vos, A. M., Mulkerrin, M. G., Clauser, K. R. & Wells, J. A. (1991) *Science* **254,** 821–825.
24. Van Ostade, X., Tavernier, J., Prangé, T. & Fiers, W. (1991) *EMBO J.* **10,** 827–836.
25. Banner, D. W., D'Arcy, A., Janes, W., Gentz, R., Schoenfeld, H.-J., Broger, C., Loetscher, H. & Lesslauer, W. (1993) *Cell* **73,** 431–455.
26. Budel, L., Hoogerbrugge, H., Pouwels, K., van Buitenen, C., Delwel, R., Löwenberg, B. & Touw, I. P. (1993) *J. Biol. Chem.* **268,** 10154–10159.
27. Murakami, M., Narazaki, M., Hibi, M., Yawata, H., Yasukawa, K., Hamaguchi, M., Taga, T. & Kishimoto, T. (1991) *Proc. Natl. Acad. Sci. USA* **88,** 11349–11353.
28. Zon, L. I., Moreau, J.-F., Koo, J.-W., Mathey-Prevot, B. & d'Andrea, A. D. (1992) *Mol. Cell. Biol.* **12,** 2949–2957.
29. Takaki, S., Murata, Y., Kitamura, T., Miyajima, A., Tominaga, A. & Takatsu, K. (1993) *J. Exp. Med.* **177,** 1523–1529.
30. Ronco, L. V., Silverman, S. L., Wong, S. G., Slamon, D. J., Park, L. S. & Gasson, J. C. (1994) *J. Biol. Chem.* **269,** 277–283.
31. Lopez, A., Shannon, M. F., Hercus, T., Nicola, N., Cambareri, B., Dottore, M., Layton, M. J., Eglinton, L. & Vadas, M. A. (1992) *EMBO J.* **11,** 909–916.
32. Shanafelt, A. B., Miyajima, A., Kitamura, T. & Kastelein, R. A. (1991) *EMBO J.* **10,** 4105–4112.
33. Lopez, A., Shannon, M. F., Barry, S., Phillips, J. A., Cambareri, B., Dottore, M., Simmons, P. & Vadas, M. A. (1992) *Proc Natl. Acad. Sci. USA* **89,** 11842–11846.
34. Shanafelt, A. B. & Kastelein, R. A. (1992) *J. Biol. Chem.* **267** 25466–25472.